Nematic and smectic order in a fluid of biaxial hard particles

Mark P. Taylor*
Department of Chemistry, Brandeis University, Waltham, Massachusetts 02254-9110
and Department of Physics, Brandeis University, Waltham, Massachusetts 02254-9110

Judith Herzfeld
Department of Chemistry, Brandeis University, Waltham, Massachusetts 02254-9110
(Received 16 August 1990; revised manuscript received 13 May 1991)

The liquid-crystalline phase behavior of a fluid of biaxial hard particles (spheroplatelets) is studied using a scaled particle calculation of the fluid configurational entropy combined with a cell description of translational order. If translational ordering is ignored, the density versus particle biaxiality phase diagram displays a cusp-shaped biaxial-nematic phase intervening between two uniaxial nematic phases. The location of the crossover from rodlike to platelike uniaxial-nematic behavior is in agreement with previous bifurcation-analysis results. The density discontinuity at the isotropic-nematic transition decreases as this crossover is approached from both the rodlike and platelike sides, becoming vanishingly small at the crossover point itself. When the possibility of translational order is considered, the phase diagram displays three distinct smectic-A phases, in addition to the two uniaxial nematic phases, and only a small remnant of the biaxial-nematic phase. One of the three smectic phases has in-layer orientational order, while the other two have in-layer isotropic order.

INTRODUCTION

The term *liquid crystal* encompasses a broad range of fluid materials displaying anisotropic properties and ordered mesophases. On a microscopic level all of these materials are characterized by a significant degree of molecular shape anisotropy [1], a fact which suggests that liquid-crystalline order may be understood in terms of a fluid of asymmetric hard particles [2]. Uniaxial-hard-particle models have been studied extensively and appear to provide a reasonable qualitative description of a variety of liquid-crystal phases [2–9]. However, quantitatively, such uniaxial-hard-particle models give results systematically at odds with experimental findings. Specifically, the uniaxial-hard-particle model generally overestimates the nematic order parameter and gives exaggerated discontinuities in density, entropy, and enthalpy across the isotropic-nematic transition. Such discrepancies persist even when attractive interparticle interactions are included in the hard-core description (i.e., the van der Waals approach) [10].

It has been suggested that a fluid of hard biaxial particles should provide a more realistic reference system for mesogenic fluids than does a fluid of hard uniaxial particles [10,11]. This suggestion is prompted primarily by the fact that, on a molecular level, most mesogenic molecules are by no means uniaxially symmetric. On a macroscopic level this approach seems promising since, as pointed out by Gelbart and Barboy [11] (and more recently by Tjipto-Margo and Evans [12]), introduction of a small degree of biaxiality into the hard particle model can result in more realistic nematic behavior (such as an order of magnitude decrease in the isotropic-nematic transition density discontinuity). Fluids governed by an underlying biaxial interparticle potential have been of considerable interest and are predicted to have a complex phase diagram which includes one biaxial- and two uniaxial-nematic phases [13–18]. In a density versus particle biaxiality phase diagram first described by Alben [15] the uniaxial-nematic phases for rodlike and platelike particles are separated from the intervening biaxial phase by two second-order transition lines which meet the first-order isotropic-nematic phase boundary in a sharp cusp. This intersection, at which four phases coexist, is a distinguishing feature of the phase diagram and is known as the Landau bicritical point. Preliminary results from recent computer simulations of a fluid of hard biaxial ellipsoids include a phase diagram of this very topology [19].

The prediction of a stable biaxial-nematic phase in these model biaxial systems has raised some questions as to their applicability to real systems as there are remarkably few experimental systems for which such a phase has been identified [20–22]. One possible explanation for this near nonexistence of the biaxial-nematic phase is provided by recent studies of certain uniaxial-hard-particle fluids [8,9] for which the nematic phase is unstable, above a critical density, with respect to other more highly ordered liquid-crystalline phases, e.g., the smectic in a dense fluid of spherocylinders. It has been suggested that, at least in certain hard particle biaxial systems, the biaxial-nematic phase is likewise unstable with respect to smectic ordering [17,18]. (Of course this argument does not apply to ellipsoids as uniaxial ellipsoids do *not* form a smectic phase [7] and a biaxial-nematic phase *is* stable in a fluid of biaxial ellipsoids [19]). Somoza and Tarazona have used a density-functional theory to study one such biaxial-hard-particle system, a fluid of oblique cylinders, and find stable smectic ordering with only a small region of biaxial-nematic stability [23].

Here we study both nematic and smectic order in a fluid of hard biaxial spheroplatelets. We use scaled parti-

cle theory for the fluid configurational entropy [24], in conjunction with a cell description of translational order [25]. For an isotropic distribution of spheroplatelets the exact scaled particle theory results are given. However, in our description of nematic and smectic order we resort to the simplifying *xyz* approximation whereby particles are constrained to a discrete set of three mutually orthogonal orientations [26]. This approximation reproduces the well-known biaxial phase behavior described above in the absence of translation ordering (although an actual bicritical point is not found). The location of the axial-to-planar nematic crossover is in agreement with the previous spheroplatelet calculations of Mulder using a second virial treatment [17] and Holyst and Poniewierski using a density-functional theory [18]. When smectic ordering is considered, the biaxial spheroplatelet phase diagram displays three distinct smectic-A phases which almost completely displace the biaxial-nematic phase. One of the three smectic phases has in-layer orientational order while the other two have in-layer isotropic order. We also find that these smectic phases are stable with respect to both columnar and crystalline ordering.

NEMATIC ORDER

We begin by working out the general scaled particle theory equations for a fluid of hard biaxial particles. For an isotropic distribution of such particles the exact solution to these equations is presented. For calculations of the full phase diagram, these equations are solved within the discrete orientation *xyz* approximation. The biaxial particle we consider is the spheroplatelet, which is the geometrical object swept out by a sphere of radius a whose center is constrained to a rectangle of dimensions $b \times c$ $(0<b<c)$. This particle is the only nonaxially symmetric convex body for which the pair excluded volume at arbitrary fixed orientations is known in closed form [27]. Our model system consists of N hard spheroplatelets of dimensions a,b,c [particle volume $v_0=4\pi a^3/3+\pi a^2(b+c)+2abc$] in a volume V, with orientational order described by f_Ω, the fraction of particles with orientation Ω such that $\sum_\Omega f_\Omega=1$. The particle orientation is defined here, with respect to a fixed laboratory frame, by the particle principle axes $\Omega=\{\hat{\mathbf{u}}_a,\hat{\mathbf{u}}_b,\hat{\mathbf{u}}_c\}=\{\Omega_a,\Omega_b,\Omega_c\}$, where $\hat{\mathbf{u}}_a$ defines the normal to the basis platelet, i.e., the a axis and $\hat{\mathbf{u}}_b$ and $\hat{\mathbf{u}}_c$ refer to the b and c axes, respectively. Clearly the specification of two principle axes fixes the third, however, in the following we refer to the orientations of all three axes for clarity.

We use scaled particle theory, in the manner of Cotter [4] and of Savithramma and Madhusudana [28], to describe this spheroplatelet fluid. Required is the work function $W_\Omega(\delta_a,\delta_b,\delta_c)$ associated with the insertion of a scaled spheroplatelet of dimensions $\delta_a a$, $\delta_b b$, $\delta_c c$ $(0\le\delta_a,\delta_b,\delta_c<\infty)$ and orientation Ω in this fluid of (a,b,c) spheroplatelets. This quantity is known exactly for the two limiting cases of a vanishingly small and of a macroscopically large scaled particle. In the former limit, this work function is given by

$$\beta W_\Omega(\delta_a,\delta_b,\delta_c\to 0)=-\ln\left[1-\rho\sum_{\Omega'}f_{\Omega'}b^{\rm ex}_{\Omega,\Omega'}(\delta_a,\delta_b,\delta_c)\right]$$
$$=-\ln[1-\rho\langle b^{\rm ex}_{\Omega,\Omega'}(\delta_a,\delta_b,\delta_c)\rangle] \tag{1}$$

where $\beta=1/k_BT$, $\rho=N/V$, and $b^{\rm ex}_{\Omega,\Omega'}(\delta_a,\delta_b,\delta_c)$ is the pair excluded volume between the scaled $(\delta_a a,\delta_b b,\delta_c c)$ spheroplatelet in orientation Ω and an (a,b,c) spheroplatelet in orientation Ω'. We have also introduced the notation $\langle g_\Omega\rangle=\sum_\Omega f_\Omega g_\Omega$, which we shall use throughout. The explicit form of the pair excluded volume, as given by Taylor [29], is

$$b^{\rm ex}_{\Omega,\Omega'}(\delta_a,\delta_b,\delta_c)=\frac{4\pi}{3}a^3(1+\delta_a)^3+\pi a^2b(1+\delta_a)^2(1+\delta_b)+\pi a^2c(1+\delta_a)^2(1+\delta_c)+2abc(1+\delta_a)(1+\delta_b\delta_c)$$
$$+2abc(1+\delta_a)\delta_c|\sin(\Omega_b-\Omega'_c)|+2abc(1+\delta_a)\delta_b|\sin(\Omega_c-\Omega'_b)|$$
$$+2ab^2(1+\delta_a)\delta_b|\sin(\Omega_b-\Omega'_b)|+2ac^2(1+\delta_a)\delta_c|\sin(\Omega_c-\Omega'_c)|$$
$$+b^2c\delta_b[|\cos(\Omega_a-\Omega'_b)|+\delta_c|\cos(\Omega_b-\Omega'_a)|]+bc^2\delta_c[|\cos(\Omega_a-\Omega'_c)|+\delta_b|\cos(\Omega_c-\Omega'_a)|]\ . \tag{2}$$

Note that the argument of the logarithm in Eq. (1) is simply the probability of success in the insertion process in the $\delta_a,\delta_b,\delta_c\to 0$ limit. In the other limit of a macroscopically large scaled particle $(\delta_a,\delta_b,\delta_c\to\infty)$, the work function is given simply in terms of a hydrostatic pressure P resisting the formation of a macroscopic cavity in the fluid, i.e.,

$$\beta W_\Omega(\delta_a,\delta_b,\delta_c\to\infty)=\beta P\left[\left[\frac{4\pi}{3}a^3\right]\delta_a^3+(\pi a^2b)\delta_a^2\delta_b+(\pi a^2c)\delta_a^2\delta_c+(2abc)\delta_a\delta_b\delta_c\right]\ . \tag{3}$$

The premise of scaled particle theory is that the work function for the case of interest, $\delta_a,\delta_b,\delta_c=1$, can be approximated by an interpolation between these two exact limiting cases. Such an interpolation is constructed through an expansion of the orientationally averaged work function in the scaling parameters $\delta_a,\delta_b,\delta_c$ as follows:

$$\beta W(\delta_a,\delta_b,\delta_c)=\sum_\Omega f_\Omega \beta W_\Omega(\delta_a,\delta_b,\delta_c)$$
$$=C_{000}+C_{100}\delta_a+C_{010}\delta_b+C_{001}\delta_c+C_{110}\delta_a\delta_b+C_{101}\delta_a\delta_c$$
$$+C_{011}\delta_b\delta_c+C_{200}\delta_a^2+\pi a^2 b(\beta P)\delta_a^2\delta_b+\pi a^2 c(\beta P)\delta_a^2\delta_c+2abc(\beta P)\delta_a\delta_b\delta_c+\frac{4\pi}{3}a^3(\beta P)\delta_a^3 \tag{4}$$

where the expansion coefficients

$$C_{lmn}=\frac{1}{l!m!n!}\left[\frac{\partial^{(l+m+n)}(\beta W)}{\partial\delta_a^l\partial\delta_b^m\partial\delta_c^n}\right]_{\delta_a,\delta_b,\delta_c=0} \tag{5}$$

are computed using the small scaling limit work function from Eq. (1):

$$\beta W(\delta_a,\delta_b,\delta_c\to 0)=\sum_\Omega f_\Omega \beta W_\Omega(\delta_a,\delta_b,\delta_c\to 0)$$
$$=-\ln\left[\prod_\Omega\left[1-\rho\sum_{\Omega'}f_{\Omega'}b^{\rm ex}_{\Omega,\Omega'}(\delta_a,\delta_b,\delta_c)\right]^{f_\Omega}\right]$$
$$\approx-\ln[1-\rho\langle\langle\, b^{\rm ex}_{\Omega,\Omega'}(\delta_a,\delta_b,\delta_c)\,\rangle\rangle]\ . \tag{6}$$

Evaluation of the C_{lmn} expansion coefficients leads to the desired $\delta_a,\delta_b,\delta_c=1$ orientationally averaged work function,

$$\beta W(\delta_a,\delta_b,\delta_c=1)=-\ln(1-v_p)+\frac{\mathcal{B}}{v_0}\left[\frac{v_p}{1-v_p}\right]+\frac{\mathcal{C}}{v_0^2}\left[\frac{v_p}{1-v_p}\right]^2+v_0\beta P \tag{7}$$

where

$$\mathcal{B}=8\pi a^3+6\pi a^2 b+6\pi a^2 c+4abc+4abc\langle\langle\,|\sin(\Omega_b-\Omega_c')|\,\rangle\rangle+4abc\langle\langle\,|\sin(\Omega_c-\Omega_b')|\,\rangle\rangle$$
$$+4ab^2\langle\langle\,|\sin(\Omega_b-\Omega_b')|\,\rangle\rangle+4ac^2\langle\langle\,|\sin(\Omega_c-\Omega_c')|\,\rangle\rangle+b^2c[\langle\langle\,|\cos(\Omega_a-\Omega_b')|\,\rangle\rangle+\langle\langle\,|\cos(\Omega_b-\Omega_a')|\,\rangle\rangle]$$
$$+bc^2[\langle\langle\,|\cos(\Omega_a-\Omega_c')|\,\rangle\rangle+\langle\langle\,|\cos(\Omega_c-\Omega_a')|\,\rangle\rangle]\ , \tag{8}$$

$$\mathcal{C}=(4\pi a^3+2\pi a^2 b+2\pi a^2 c+2abc)$$
$$\times[2\pi a^3+2\pi a^2 b+2\pi a^2 c+abc+2abc\langle\langle\,|\sin(\Omega_b-\Omega_c')|\,\rangle\rangle+2abc\langle\langle\,|\sin(\Omega_c-\Omega_b')|\,\rangle\rangle$$
$$+2ab^2\langle\langle\,|\sin(\Omega_b-\Omega_b')|\,\rangle\rangle+2ac^2\langle\langle\,|\sin(\Omega_c-\Omega_c')|\,\rangle\rangle+b^2c\langle\langle\,|\cos(\Omega_a-\Omega_b')|\,\rangle\rangle+bc^2\langle\langle\,|\cos(\Omega_a-\Omega_c')|\,\rangle\rangle]$$
$$+[\pi a^2 b+2abc\langle\langle\,|\sin(\Omega_c-\Omega_b')|\,\rangle\rangle+2ab^2\langle\langle\,|\sin(\Omega_b-\Omega_b')|\,\rangle\rangle+b^2c\langle\langle\,|\cos(\Omega_a-\Omega_b')|\,\rangle\rangle]$$
$$\times[\pi a^2 c+2abc\langle\langle\,|\sin(\Omega_b-\Omega_c')|\,\rangle\rangle+2ac^2\langle\langle\,|\sin(\Omega_c-\Omega_c')|\,\rangle\rangle+bc^2\langle\langle\,|\cos(\Omega_a-\Omega_c')|\,\rangle\rangle] \tag{9}$$

and $v_p=\rho v_0$ is the volume or packing fraction of particles.

The complete thermodynamics of this hard particle fluid can be constructed from the Eq. (7) work function. The Gibbs free energy is given by

$$\frac{\beta G[f_\Omega]}{N}=\langle\ln f_\Omega\rangle+\ln(\rho\Lambda^3)+\beta W(\delta_a,\delta_b,\delta_c=1) \tag{10}$$

where $\Lambda=(h^2/2\pi m k_B T)^{1/2}$ is the thermal de Broglie wavelength for a particle of mass m. Integration of the Gibbs-Duhem equation, $\partial P/\partial\rho=\rho\partial(G/N)/\partial\rho$, gives the pressure equation of state

$$v_0\beta P=\frac{v_p}{1-v_p}+\frac{\mathcal{B}}{2v_0}\left[\frac{v_p}{1-v_p}\right]^2+\frac{2\mathcal{C}}{3v_0^2}\left[\frac{v_p}{1-v_p}\right]^3 \tag{11}$$

and the Helmholtz free energy is

$$\frac{\beta F[f_\Omega]}{N}=\frac{\beta G}{N}-\frac{v_0\beta P}{v_p}$$
$$=\langle\ln f_\Omega\rangle-1+\ln(\rho\Lambda^3)-\ln(1-v_p)$$
$$+\frac{\mathcal{B}}{2v_0}\left[\frac{v_p}{1-v_p}\right]+\frac{\mathcal{C}}{3v_0^2}\left[\frac{v_p}{1-v_p}\right]^2\ . \tag{12}$$

This version of scaled particle theory reproduces both the original results of Reiss, Frisch, and Lebowitz for the hard sphere fluid ($b,c=0$) [24] and those of Cotter for hard spherocylinders ($b=0$) [4].

For an isotropic fluid of spheroplatelets, the orientation distribution function f_Ω is simply a constant and the angular averages of Eqs. (8) and (9) are given by $\langle\langle\,|\sin(\Omega_\alpha-\Omega_\gamma')|\,\rangle\rangle=\pi/4$ and $\langle\langle\,|\cos(\Omega_\alpha-\Omega_\gamma')|\,\rangle\rangle=\frac{1}{2}$, $\alpha,\gamma\in\{a,b,c\}$ [27]. Thus for the isotropic solution we have

$$\mathcal{B}^{\rm iso}=8\pi a^3+6\pi a^2(b+c)+4abc+\pi a(b+c)^2+bc(b+c) \tag{13}$$

and

$$\mathcal{C}^{\rm iso}\frac{1}{4a^3}[8a^3+4a^2(b+c)+abc] \times[2\pi a^3+\pi a^2(b+c)+abc]^2 . \tag{14}$$

The resulting second virial coefficient for hard spheroplatelets is given by $B_2=v_0+\frac{1}{2}\mathcal{B}^{\rm iso}$ in agreement with Mulder's result [27]. This scaled particle theory approach gives a third virial coefficient of $B_3=v_0^2+v_0\mathcal{B}^{\rm iso}+\frac{2}{3}\mathcal{C}^{\rm iso}$ and, in general, the nth virial coefficient is determined from Eq. (11) via

$$B_{n+1}=\frac{v_0^n}{n!}\frac{\partial^n(v_0\beta P/v_p)}{\partial v_p^n}\bigg|_{v_p=0} . \tag{15}$$

In the nematic phase the orientation distribution function is no longer a constant and is determined via a functional minimization of the Helmholtz free energy [Eq. (12)] with respect to f_Ω. The minimization condition, given by

$$\frac{\delta(\beta F[f_\Omega]/N+\chi\sum_\Omega f_\Omega)}{\delta f_\Omega}=0 \tag{16}$$

where χ is a Lagrange multiplier conjugate to the f_Ω normalization constraint, results in a rather complicated nonlinear integral equation for the equilibrium orientation distribution function. Here we make no attempt to solve this full integral equation. Instead, we resort to a discretized version of the above model in which particle orientations are restricted, such that the particle principle axes are constrained to coincide with the axes of a fixed Cartesian xyz-coordinate system. Systems of hard rectangular biaxial particles have been studied within this approximation by both Shih and Alben using a lattice model [14] and Gelbart and Barboy using their y expansion [11(a)]. Somoza and Tarazona also employ such a discrete orientation approximation for oblique hard cylinders [23]. While not quantitatively accurate [30], the xyz approach should provide a qualitative description of this biaxial system. We note here that within this xyz approximation the results we derive for spheroplatelets are qualitatively very similar to results we get if we simply use hard rectangular particles. However, use of the spheroplatelet allows assessment of the xyz approximation by comparison with analytical and numerical results regarding the location of the Landau bicritical point in the spheroplatelet fluid [17,18] and exact computer simulation results in the limit of $b=0$ (i.e., spherocylinders) [8].

A discrete version of the orientation distribution function f_{jk} is defined as the fraction of particles with principle axes $\hat{\mathbf{u}}_a$, $\hat{\mathbf{u}}_b$, and $\hat{\mathbf{u}}_c$ oriented in fixed directions i, j, and k, respectively. Note that a biaxial particle has six distinct orientations in the xyz approximation ($i\neq j\neq k$). Averages over the distribution function are defined by $\langle g_{jk}\rangle=\sum_{j\neq k}f_{jk}g_{jk}$, where the sum extends over all six pairs (j,k) for which $j\neq k$. In this xyz approximation,

$$|\sin(\Omega_b-\Omega_c')|=(1-\delta_{jk'}) , \quad |\sin(\Omega_c-\Omega_b')|=(1-\delta_{kj'}) ,$$
$$|\sin(\Omega_b-\Omega_b')|=(1-\delta_{jj'}) , \quad |\sin(\Omega_c-\Omega_c')|=(1-\delta_{kk'}) ,$$
$$|\cos(\Omega_a-\Omega_b')|=(1-\delta_{ij'})=(1-\delta_{jj'}-\delta_{kj'}) , \quad |\cos(\Omega_b-\Omega_a')|=(1-\delta_{ji'})=(1-\delta_{jj'}-\delta_{jk'}) ,$$
$$|\cos(\Omega_a-\Omega_c')|=(1-\delta_{ik'})=(1-\delta_{jk'}-\delta_{kk'}) , \quad |\cos(\Omega_c-\Omega_a')|=(1-\delta_{ki'})=(1-\delta_{jk'}-\delta_{kk'}) ,$$

where $\delta_{jk'}$ is the usual Kronecker δ function, and the above-mentioned nonlinear integral equation is reduced to a set of seven coupled algebraic equations. This set of equations can be solved using the Newton-Raphson technique or, more directly, by using a straightforward iterative procedure. We consider solutions of four different symmetries defined as follows:

$f_{23}=f_{13}=f_{32}=f_{31}=f_{12}=f_{21}$, isotropic,

$(f_{23}=f_{13})>(f_{32}=f_{31})>(f_{12}=f_{21})$, rodlike uniaxial nematic, $N_u(+)$,

$f_{23}>f_{13}>f_{32}>f_{31}>f_{12}>f_{21}$
$f_{23}>(f_{13}=f_{32})>(f_{31}=f_{12})>f_{21}$
$f_{23}>f_{32}>f_{13}>f_{12}>f_{31}>f_{21}$ } biaxial nematic, N_{bx} ,

$(f_{23}=f_{32})>(f_{13}=f_{12})>(f_{31}=f_{21})$, platelike uniaxial nematic, $N_u(-)$.

For the rodlike uniaxial nematic, $N_u(+)$, the director is along direction 3 and particle orientations with the longest axis (c) parallel to the director are most populated while those with the shortest axis (a) parallel to the director are least populated. For the platelike uniaxial nematic, $N_u(-)$, the director is along direction 1 and particle orientations with the shortest axis (a) along the director are most populated while those with the longest axis (c)

along the director are least populated. These two uniaxial nematics can be connected in a continuous manner by passing through the biaxial nematic, N_{bx}.

The phase diagram for the $c/2a=5$ spheroplatelet fluid resulting from this calculation is shown in Fig. 1. A corresponding plot of the relative density discontinuity across the isotropic-nematic transition is shown in Fig. 2. In the phase diagram, a cusp-shaped region of biaxial nematic stability, N_{bx}, separates two uniaxial nematics, the rodlike $N_u(+)$, in which the particles' long axes are aligned along the nematic director, and the platelike $N_u(-)$, in which the particles' short axes are aligned along the director. The uniaxial- to biaxial-nematic transition is, in all cases, apparently second order ($\Delta\rho/\rho<10^{-4}$). The crossover from $N_u(+)$ to $N_u(-)$ behavior occurs at a particle biaxiality of $b/2a=1.35$ which is in agreement with the bifurcation analysis condition given by $b^2+\pi ba-\pi ca/2=0$ [17,18] where in our case, $c/2a=5$. (In fact, our values of $b/2a$ at the crossover are consistent with this bifurcation analysis result for all values of $c/2a$ investigated.) The density discontinuity at the first-order isotropic-nematic transition (Fig. 2) decreases as this crossover point is approached from both the rodlike and platelike sides, becoming vanishingly small ($\Delta\rho/\rho<10^{-4}$) at the crossover.

The effects of the discrete orientation (xyz) approximation are most strongly manifest at the rotational symmetry breaking, isotropic-nematic transition. This transition occurs prematurely due to an underestimation of orientational disorder in the isotropic phase and a lesser overestimation of orientational order in the nematic phase. For comparison, this transition is known to occur at $\rho v_0\approx 0.40$ for spherocylinders (i.e., $b=0$) [8] with $c/2a=5$ while the bicritical point for this $c/2a$ value is estimated to occur at $\rho v_0=0.43$ [18]. A consequence of our underestimation of the isotropic-nematic transition density is the absence of a bicritical point in the Fig. 1 phase diagram, where the N_{bx} phase terminates at $\rho v_0=0.34$ rather than extending down to the $\rho v_0=0.25$ isotropic-nematic transition boundary. However, apart from the location of the isotropic-nematic transition, the overall description of this transition and of the complete nematic phase behavior for the spheroplatelet fluid is qualitatively [and even quantitatively, in the case of the $N_u(+)\rightarrow N_u(-)$ crossover condition] correct.

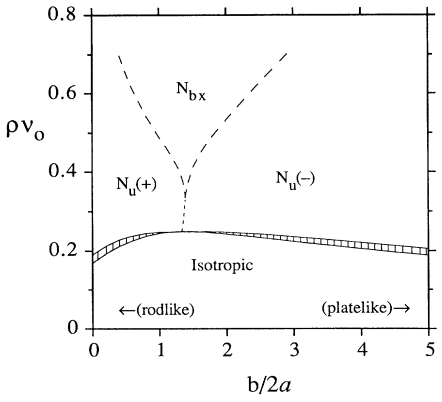

FIG. 1. Phase diagram for a fluid of hard spheroplatelets with $c/2a=5$ computed using an xyz version of scaled particle theory. Broken lines indicate second-order phase transitions while shaded areas denote regions of first-order phase coexistence. The three aligned phases are the axial nematic $N_u(+)$, the planar nematic $N_u(-)$, and the biaxial nematic N_{bx}.

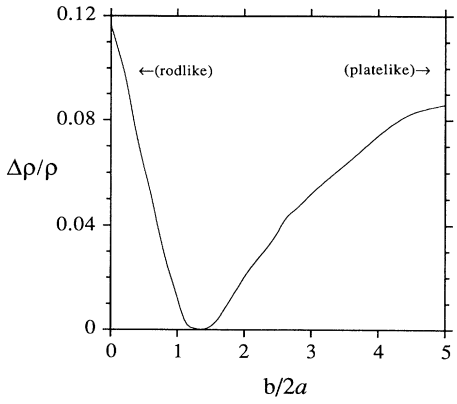

FIG. 2. Relative density discontinuity across the isotropic-nematic transition $\Delta\rho/\rho$ vs $b/2a$ for a fluid of hard spheroplatelets with $c/2a=5$ (corresponding to the spheroplatelet phase diagram of Fig. 1). At the crossover from rodlike to platelike behavior ($b/2a=1.35$) the density discontinuity becomes vanishingly small ($\Delta\rho/\rho<10^{-4}$) suggesting a second-order alignment transition at this point.

SMECTIC ORDER

Our xyz treatment of the nematic order in a fluid of biaxial hard particles results in a familiar phase diagram including the previously predicted biaxial-nematic phase. However, as discussed in the Introduction, the fact that such a biaxial-nematic phase is rarely seen experimentally casts doubt on the applicability of this type of model. The discovery of a stable smectic phase in a fluid of uniaxial spherocylinders [8] has led to the suggestion that, at least in certain hard particle systems, the elusive biaxial-nematic phase is actually unstable with respect to smectic ordering [17,18,23]. If this is the case, the region of biaxial-nematic stability in the Fig. 1 biaxial spheroplatelet phase diagram should actually be replaced by a more stable, smectic phase. Here we investigate the question of smectic ordering in a biaxial spheroplatelet fluid using a self-consistent cell model for translational order in hard particle fluids [25].

In this model, smectic order is imposed by the introduction of impenetrable cell walls which divide the system into smectic layers. The smectic phase is thus treated as a two-dimensional fluid confined within the one-

dimensional cell corresponding to the thickness of the smectic layer. The two-dimensional fluid density is coupled to the one-dimensional cell entropy through their mutual dependence on the smectic layer spacing Δ_s. For self-consistency this model requires that one of the spheroplatelet principle axes ($\hat{\mathbf{u}}_a,\hat{\mathbf{u}}_b,\hat{\mathbf{u}}_c$) be constrained to lie parallel to the smectic ordering axis ($\hat{\mathbf{m}}$), however, the particles still retain in-layer rotational freedom [31]. This construction allows for three types of smectic-A ordering, depending on which of the three spheroplatelet principle axes is associated with the smectic ordering axis. In addition, there can be either isotropic or nematic in-layer ordering.

Following the approach developed in Ref. [25], the free energy per particle for this system can be written as the sum of three terms, an ideal contribution,

$$\beta F^{\text{ideal}}/N=\sum_{\Omega} f_{\Omega}\ln f_{\Omega}+\ln\rho\Lambda^3-1 \tag{17}$$

and the two nonideal contributions, $\beta F_1^{\text{cryst}}/N$ and $\beta F_2^{\text{fluid}}/N$, associated with the one ordered and two disordered (fluid) dimensions of the system, respectively. In the one translationally ordered dimension, defined by the smectic ordering axis, we describe the system in terms of one-dimensional particles of length l confined within one-dimensional cells of length Δ_s where

$$l=\begin{cases}2a & \text{for } \hat{\mathbf{m}}=\hat{\mathbf{u}}_a\\ 2a+b & \text{for } \hat{\mathbf{m}}=\hat{\mathbf{u}}_b\\ 2a+c & \text{for } \hat{\mathbf{m}}=\hat{\mathbf{u}}_c\ .\end{cases} \tag{18}$$

The one-dimensional cell entropy per particle is simply $\ln(\Gamma/\Delta_s)$ where $\Gamma=\Delta_s-l$ is the free "volume" accessible to the center of a confined particle and thus

$$\beta F_1^{\text{cryst}}/N=-\ln(1-l/\Delta_s)\ . \tag{19}$$

In the remaining two translationally disordered (in-layer) dimensions we have a corresponding two-dimensional fluid of N two-dimensional particles in a total area V/Δ_s. We first consider the case in which $\hat{\mathbf{m}}=\hat{\mathbf{u}}_a$ (i.e., the particles' a axes are parallel to the smectic ordering axis). In this case, the shape of the two-dimensional particles, here referred to as "circloplatelets," is given by the parallel projection of an (a,b,c) spheroplatelet on a plane perpendicular to the a axis [particle area $\omega_0=\pi a^2+2a(b+c)+bc$]. This two-dimensional fluid is described using a two-dimensional version of scaled particle theory. For this purpose we consider the process of inserting a scaled circloplatelet of dimensions $\delta_a a$, $\delta_b b$, $\delta_c c$ and orientation Ω (which is now defined in terms of a single angle) into this two-dimensional fluid of (a,b,c) circloplatelets. In the limit of a vanishingly small scaled particle, the work associated with this process is given exactly by

$$\beta W_{\Omega}(\delta_a,\delta_b,\delta_c\to 0)=-\ln\left[1-\rho\Delta_s\sum_{\Omega'} f_{\Omega'}A_{\Omega,\Omega'}(\delta_a,\delta_b,\delta_c)\right] \tag{20}$$

where

$$\begin{aligned}A_{\Omega,\Omega'}(\delta_a,\delta_b,\delta_c)=&\pi a^2(1+\delta_a)^2+2ab(1+\delta_a)(1+\delta_b)+2ac(1+\delta_a)(1+\delta_c)+cb(1+\delta_b\delta_c)\\&+cb(\delta_b+\delta_c)|\cos(\Omega-\Omega')|+(c^2\delta_c+b^2\delta_b)|\sin(\Omega-\Omega')|\end{aligned} \tag{21}$$

is the excluded area between the scaled $(\delta_a a,\delta_b b,\delta_c c)$ circloplatelet in orientation Ω and an (a,b,c) circloplatelet in orientation Ω'. In the limit of a macroscopically large scaled particle ($\delta_a,\delta_b,\delta_c\to\infty$), this work function is given exactly in terms of a two-dimensional pressure Π. We interpolate between these two limits via an expansion in the scaling parameters as follows:

$$\begin{aligned}\beta W(\delta_a,\delta_b,\delta_c)=&\sum_{\Omega} f_{\Omega}\beta W_{\Omega}(\delta_a,\delta_b,\delta_c)\\=&C_{000}+C_{100}\delta_a+C_{010}\delta_b+C_{001}\delta_c+\pi a^2(\beta\Pi)\delta_a^2+2ab(\beta\Pi)\delta_a\delta_b+2ac(\beta\Pi)\delta_a\delta_c+bc(\beta\Pi)\delta_b\delta_c\end{aligned} \tag{22}$$

where the expansion coefficients C_{lmn}, given by Eq. (5), are computed using an orientationally averaged [as in Eq. (6)] version of the small scaling limit work function [Eq. (20)].

Construction of the analogous scaled particle work function for the $\hat{\mathbf{m}}=\hat{\mathbf{u}}_b$ and $\hat{\mathbf{m}}=\hat{\mathbf{u}}_c$ smectic structures exactly parallels the above derivation. For these two cases the two-dimensional fluid of interest is composed of "circlorectangles," i.e., rectangles of length c or b capped by hemicircles of radius a ($\omega_0=\pi a^2+2ac$ or $\omega_0=\pi a^2+2ab$). Thus only two scaling parameters are required, one for the rectangle length (δ_c or δ_b) and one for the circle radius (δ_a). For the $\hat{\mathbf{m}}=\hat{\mathbf{u}}_b$ smectic phase the excluded area [analogous to Eq. (21)] and work function [analogous to Eq. (22)] are given, respectively, by

$$A_{\Omega,\Omega'}(\delta_a,\delta_c)=\pi a^2(1+\delta_a)^2+2ac(1+\delta_a)(1+\delta_c)+c^2\delta_c|\sin(\Omega-\Omega')| \tag{23}$$

and

$$\beta W(\delta_a,\delta_c)=C_{00}+C_{10}\delta_a+C_{01}\delta_c+\pi a^2(\beta\Pi)\delta_a^2+2ac(\beta\Pi)\delta_a\delta_c\ . \tag{24}$$

The related expressions for the $\hat{\mathbf{m}}=\hat{\mathbf{u}}_c$ smectic phase are identical to Eqs. (23) and (24) when c and δ_c are replaced by b and δ_b. The expansion coefficients of Eq. (24) are given by a suitably modified version of Eq. (5).

Proceeding with the straightforward scaled particle approach (as described above and in Ref. [25]) for each of these three smectic-A phases results in the following two-dimensional excess fluid configurational free energy:

$$\beta F_2^{\text{fluid}}/N=-\ln(1-v_2)+\frac{\mathcal{B}}{2\omega_0}\left[\frac{v_2}{1-v_2}\right] \tag{25}$$

where

$$\mathcal{B}=\begin{cases}2\omega_0+(b^2+c^2)\langle\langle\,|\sin(\Omega-\Omega')|\,\rangle\rangle+2bc[\,\langle\langle\,|\cos(\Omega-\Omega'|\,\rangle\rangle-1\,] & \text{for } \hat{\mathbf{m}}=\hat{\mathbf{u}}_a\\ 2\omega_0+c^2\langle\langle\,|\sin(\Omega-\Omega')|\,\rangle\rangle & \text{for } \hat{\mathbf{m}}=\hat{\mathbf{u}}_b\\ 2\omega_0+b^2\langle\langle\,|\sin(\Omega-\Omega')|\,\rangle\rangle & \text{for } \hat{\mathbf{m}}=\hat{\mathbf{u}}_c\end{cases} \tag{26}$$

and $v_2=\omega_0\Delta_s\rho$ is the two-dimensional in-layer packing fraction with the two-dimensional particle area given by

$$\omega_0=\begin{cases}\pi a^2+2a(b+c)+bc & \text{for } \hat{\mathbf{m}}=\hat{\mathbf{u}}_a\\ \pi a^2+2ac & \text{for } \hat{\mathbf{m}}=\hat{\mathbf{u}}_b\\ \pi a^2+2ab & \text{for } \hat{\mathbf{m}}=\hat{\mathbf{u}}_c\ .\end{cases} \tag{27}$$

The complete free energy per particle, given by the sum of Eqs. (17), (19), and (25), for each of the three smectic phases is a functional of both the in-layer orientation distribution function f_Ω and the smectic layer spacing Δ_s. To be consistent with our previous xyz treatment of nematic ordering in this system, here we consider only the xy version of the in-layer orientation distribution function replacing f_Ω by f_i where $i=1,2$. This leads to the following simplifications: $|\sin(\Omega-\Omega')|\rightarrow(1-\delta_{ij})$, $|\cos(\Omega-\Omega')|\rightarrow\delta_{ij}$, and $\langle g(\Omega)\rangle\rightarrow\langle g_i\rangle=\sum_i f_i g_i$. The equilibrium in-layer orientation distribution function and smectic layer spacing for each of these smectic phases are given by simultaneously optimizing the complete free energy functional with respect to f_i (subject to the normalization $f_1+f_2=1$) and Δ_s.

Consideration of these various smectic-A phases, in addition to the isotropic and nematic phases described above, leads to the density versus particle biaxiality phase diagram shown in Fig. 3 for $c/2a=5$. This phase diagram is markedly different from the spheroplatelet phase diagram of Fig. 1 for which translational ordering was ignored. We find stable smectic ordering across the full range of particle biaxiality for volume fractions $\rho v_0\geq 0.5$. For rodlike particles ($b\rightarrow 0$) there is a first-order transition from the $N_u(+)$ phase to the uniaxial $S_u(+)$ phase ($\hat{\mathbf{m}}=\hat{\mathbf{u}}_c$) in which the rod axes are aligned perpendicular to the smectic layers. (For spherocylinders ($b=0$) with $c/2a=5$, this transition is known to occur at $\rho v_0=0.53$ and is second order [8].) As these rodlike particles become more diaxial (larger $b/2a$) or as the density is increased (for $b/2a>1$) there is an apparently second-order, in-layer orientational ordering transition from the uniaxial $S_u(+)$ phase to the biaxial $S_{bx}(+)$ phase. In the other extreme of platelike particles ($b\rightarrow c$) there is a first-order transition from the $N_u(-)$ phase to the uniaxial $S_u(-)$ phase ($\hat{\mathbf{m}}=\hat{\mathbf{u}}_a$). In the $S_u(-)$ phase, the short axes of the particles are oriented perpendicular to the smectic layer forming a lamellar structure. With increasing density, this $S_u(-)$ phase becomes unstable with respect to the biaxial $S_{bx}(+)$ phase. At this first-order phase transition the platelike particles, which are "lying down" in the $S_u(-)$ smectic layer, simultaneously "stand up" and undergo an in-layer orientational ordering transition forming the $S_{bx}(+)$ phase. At intermediate particle biaxiality ($1.4<b/2a<2.1$) there is either a first-order $N_u(-)\rightarrow S_u(+)$ or $N_u(-)\rightarrow S_{bx}(+)$ transition. We note that the strongly discontinuous nature of these nematic-smectic transitions results from the cell construction of smectic order, which precludes the possibility of a continuous transition from the nematic [25]. However, the overall smectic phase behavior shown in Fig. 3 should be qualitatively correct.

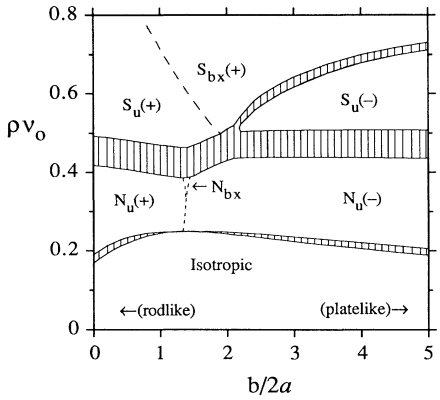

FIG. 3. Phase diagram, including smectic order, for biaxial spheroplatelets with $c/2a=5$. Broken lines indicate second-order phase transitions while shaded areas denote regions of first-order phase coexistence. The uniaxial $S_u(+)$ and $S_u(-)$ smectic phases have in-layer isotropic order while the biaxial $S_{bx}(+)$ smectic phase has in-layer nematic order. A detailed description of these smectic phases is given in the text. Of particular interest is near disappearance of the biaxial N_{bx} nematic phase (compare with Fig. 1).

Perhaps the most striking feature of the Fig. 3 phase diagram is the nearly complete disappearance of the biaxial-nematic phase. Only a small remnant of the Fig. 1 cusp-shaped region of N_{bx} stability survives, the majority of this region being replaced by the uniaxial $S_u(+)$ and biaxial $S_{bx}(+)$ phases. Due to the approximations employed here, it is unclear whether this remaining N_{bx} phase is truly stable or if the isotropic-nematic transition boundary actually merges with the nematic-smectic boundary in this region of the phase diagram. While a definitive resolution of such details awaits an "exact" computer simulation, we can conclude here that the large region of biaxial-nematic stability previously predicted for a fluid of biaxial hard particles is, for the most part, unstable with respect to smectic ordering and that if a biaxial nematic does exist in this system it is constrained to a very limited range of density and particle biaxiality.

For the case of $c/2a=5$ hard spherocylinders (i.e., $b=0$), it is known that above a density of $\rho v_0 \approx 0.65$ the smectic $S_u(+)$ phase is no longer stable with respect to crystalline ordering [8]. For the biaxial spheroplatelets studied here one similarly expects the region of smectic stability shown in Fig. 3 to be replaced by a crystal phase above some critical density. Various columnar phases may also be stable at high density in this system. We have investigated the possibility of these more highly ordered phases in the biaxial spheroplatelet system, using a generalized version of our previous model for columnar and crystalline ordering in the parallel hard spherocylinder system [25] (in analogy to our above treatment of the smectic phase). In this model, the columnar phase is described as one-dimensional fluid confined within a two-dimensional cell. The one-dimensional fluid density is coupled to the two-dimensional cell entropy through their mutual dependence on the cell dimensions. For the crystal phase the cell model is applied to translational order in all three dimensions. Details of these calculations are given in the Appendix.

Figure 4 shows the resulting biaxial spheroplatelet phase diagram when columnar and crystalline ordering are considered, in addition to the smectic ordering considered in Fig. 3. For low and intermediate densities ($\rho v_0 \leq 0.6$) Fig. 4 is identical to the phase diagram of Fig. 3, while at higher densities stable columnar and crystalline phases replace the smectic ordering of Fig. 3. Of the three possible columnar phases discussed in the Appendix, only one is found to be stable. In this $C(+)$ columnar phase the spheroplatelets' long ($\hat{\mathbf{u}}_c$) axes are parallel to the columnar tube axis and the columnar tube has a stretched hexagon cross section. The crystal phase of Fig. 4 has a close-packed structure consisting of a rectangular array of interdigitated columns of face-to-face stacked spheroplatelets. Thus, as expected, columnar and crystal phases do replace smectic ordering at high densities in the biaxial spheroplatelet fluid. However, a large region of the smectic ordering shown in Fig. 3 is actually stable with respect to these more highly ordered phases and therefore our main conclusion, that smectic ordering replaces the biaxial-nematic phase for biaxial spheroplatelets, stands.

Finally, the formation of the biaxial-nematic phase can

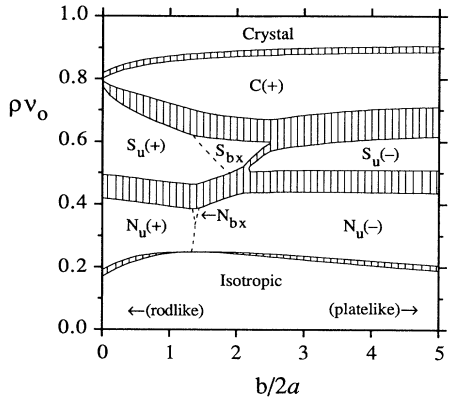

FIG. 4. Phase diagram for biaxial spheroplatelets with $c/2a=5$ as in Fig. 3, but now including columnar and crystalline ordering. The structures of these additional phases are described in the text.

be described in terms of a competition between rodlike and platelike ordering and thus a mixture of rods and plates is also predicted to exhibit such a phase [32]. One might anticipate that this mixed rod/plate biaxial-nematic phase is also unstable with respect to smectic order. However, for sufficiently incommensurate rod and plate sizes, there is the possibility of a frustration of smectic ordering and thereby a stabilization of the biaxial-nematic phase of the mixture.

ACKNOWLEDGMENTS

We gratefully acknowledge R. Hentschke for his many useful suggestions and S. Fraden for commenting on a previous version of this manuscript. This work was supported by the National Institutes of Health Grant. No. HL36546.

APPENDIX

Columnar order

Here we describe columnar ordering in the biaxial spheroplatelet system using a generalized version of the self-consistent cell model introduced in Ref. [25]. In this model columnar order is imposed by confining the particles within impenetrable columnar tubes. Thus we treat the columnar phase as a one-dimensional fluid confined within a two-dimensional cell corresponding to the cross section of the columnar tube. In analogy with the above treatment of smectic ordering, three columnar phases are possible depending upon which of the three spheroplatelet principle axes ($\hat{\mathbf{u}}_a, \hat{\mathbf{u}}_b, \hat{\mathbf{u}}_c$) is constrained to lie parallel to the columnar ordering axis ($\hat{l}$). As with the smectic phase, the free energy per particle for this system can be written as the sum of three terms, an ideal contribution, $\beta F^{\text{ideal}}/N$ given by Eq. (17) and two nonideal contributions, $\beta F_2^{\text{cryst}}/N$ and $\beta F_1^{\text{fluid}}/N$, associated with the two ordered and one disordered (fluid) dimensions of the system, respectively.

We first consider the case of $\hat{l}=\hat{\mathbf{u}}_c$ (i.e., the spheroplatelets are stacked end to end). Here, the two-dimensional cell is a hexagon of side-to-side width Δ_c which has been stretched from the midpoints of two parallel sides by a length Θ_c [two-dimensional cell area $\sigma=(\sqrt{3}/2)\Delta_c^2+\Theta_c\Delta_c$]. The two-dimensional particle confined within this cell is a circlorectangle of diameter $2a$ and rectangle length b. The free "volume" accessible to the center of this confined particle is $\Gamma=(\sqrt{3}/2)(\Delta_c-2a)^2+(\Theta_c-b)(\Delta_c-2a)$ and the nonideal contribution to the free energy associated with the two ordered dimensions is

$$\beta F_2^{\text{cryst}}/N=-\ln\left[\frac{\Gamma}{\sigma}\right] . \tag{A1}$$

In the one remaining dimension we have a fluid of one-dimensional particles of length $c+2a$ with an excess free energy given by [25]

$$\beta F_1^{\text{fluid}}/N=-\ln(1-v_1) \tag{A2}$$

where $v_1=\rho\sigma(c+2a)$ is the one-dimensional fluid density. The calculation for the $\hat{l}=\hat{\mathbf{u}}_b$ columnar phase is identical to the above if the dimensions b and c are interchanged. For the $\hat{l}=\hat{\mathbf{u}}_a$ columnar phase the spheroplatelets are stacked face to face. Here the cross section of the columnar tube is a rectangle of dimensions Δ_c by Θ_c ($\sigma=\Delta_c\Theta_c$) and the confined two-dimensional particle is an (a,b,c) circloplatelet with particle free volume $\Gamma=[\Theta_c-(c+2a)][\Delta_c-(b+2a)]$. In this phase the one-dimensional fluid density is $v_1=\rho\sigma(2a)$. For each of these three columnar phases the free energy, given by the sum of Eqs. (17), (A1), and (A2), must be minimized with respect to the cell dimensions Δ_c and Θ_c. The hard particle pressure equation of state for each of these phases is given by

$$v_0\beta P=\frac{v_p}{(1-v_1)} . \tag{A3}$$

Crystalline order

The close-packed crystal structure we consider is of a rectangular array of interdigitated columns of stacked spheroplatelets (i.e., within a column the spheroplatelets are stacked along their a axes and the b and c edges of adjacent columns are interdigitated). The close-packed volume fraction of this structure is $v_{\text{CP}}=v_0/v_{\text{cell}}$ where $v_{\text{cell}}=2abc+2\sqrt{3}a^2(b+c)+6a^3$ is the close-packed unit-cell volume. The free energy per particle of this hard particle crystal is given by [25]

$$\beta F/N=\ln\rho\Lambda^3-3\ln\left[1-\left[\frac{v_p}{v_{\text{CP}}}\right]^{1/3}\right] \tag{A4}$$

and the hard particle pressure is

$$v_0\beta P=\frac{v_p}{[1-(v_p/v_{\text{CP}})^{1/3}]} . \tag{A5}$$

*Present address: Department of Chemistry, Dartmouth College, Hanover, NH 03755.

[1] See, for example, P. G. deGennes, *The Physics of Liquid Crystals* (Clarendon, Oxford, 1974).
[2] L. Onsager, Ann. N.Y. Acad. Sci. **51**, 627 (1949).
[3] J. P. Straley, Mol. Cryst. Liq. Cryst. **22**, 333 (1973).
[4] M. A. Cotter, in *The Molecular Physics of Liquid Crystals,* edited by G. R. Luckhurst and G. W. Gray (Academic, London, 1979), Chap. 7.
[5] R. Holyst and A. Poniewierski, Mol. Phys. **68**, 381 (1989).
[6] D. Frenkel and R. Eppenga, Phys. Rev. Lett. **49**, 1089 (1982); R. Eppenga and D. Frenkel, Mol. Phys. **52**, 1303 (1984).
[7] D. Frenkel, B. M. Mulder, and J. P. McTague, Phys. Rev. Lett. **52**, 287 (1984); D. Frenkel and B. M. Mulder, Mol. Phys. **55**, 1171 (1985).
[8] D. Frenkel, H. N. W. Lekkerkerker, and A. Stroobants, Nature (London) **332**, 822 (1988); D. Frenkel, J. Phys. Chem. **92**, 3280 (1988); J. A. C. Veerman and D. Frenkel, Phys. Rev. A **41**, 3237 (1990).
[9] D. Frenkel, Liq. Cryst. **5**, 929 (1989).
[10] W. M. Gelbart, J. Phys. Chem. **86**, 4298 (1982).
[11] (a) W. M. Gelbart and B. Barboy, Acc. Chem. Res. **13**, 290 (1980); (b) Mol. Cryst. Liq. Cryst. **55**, 209 (1979).
[12] B. Tjipto-Margo and G. T. Evans, J. Chem. Phys. **94**, 4546 (1991).
[13] M. J. Freiser, Phys. Rev. Lett. **24**, 1041 (1970); Mol. Cryst. Liq. Cryst. **14**, 165 (1971).
[14] C. S. Shih and R. Alben, J. Chem. Phys. **57**, 3055 (1972).
[15] R. Alben, Phys. Rev. Lett. **30**, 778 (1973).
[16] J. P. Straley, Phys. Rev. A **10**, 1881 (1974).
[17] B. Mulder, Phys. Rev. A **39**, 360 (1989); Liq. Cryst. **8**, 527 (1990).
[18] R. Holyst and A. Poniewierski, Mol. Phys. **69**, 193 (1990).
[19] M. P. Allen, Liq. Cryst. **8**, 499 (1990).
[20] L. J. Yu and A. Saupe, Phys. Rev. Lett. **45**, 1000 (1980).
[21] S. Chandrasekhar, B. R. Ratna, B. K. Sadashiva, and V. N. Raja, Mol. Cryst. Liq. Cryst. **165**, 123 (1988).
[22] Y. Galerne, Mol. Cryst. Liq. Cryst. **165**, 131 (1988).
[23] A. M. Somoza and P. Tarazona, Phys. Rev. Lett. **61**, 2566 (1988); J. Chem. Phys. **91**, 517 (1989).
[24] H. Reiss, H. L. Frisch, and J. L. Lebowitz, J. Chem. Phys. **31**, 369 (1959); E. Helfand, H. L. Frisch, and J. L. Lebowitz, *ibid.* **34**, 1037 (1961).
[25] M. P. Taylor, R. Hentschke, and J. Herzfeld, Phys. Rev. Lett. **62**, 800 (1989); **62**, 1577(E) (1989); R. Hentschke, M. P. Taylor, and J. Herzfeld, Phys. Rev. A **40**, 1678 (1989).
[26] This type of approximation is used in Refs. [11], [14], and [23] and originated with E. A. DiMarzio, J. Chem. Phys. **35**, 658 (1961); and R. W. Zwanzig, *ibid.* **39**, 1714 (1963).
[27] B. M. Mulder, Liq. Cryst. **1**, 539 (1986).
[28] K. L. Savithramma and N. V. Madhusudana, Mol. Cryst. Liq. Cryst. **74**, 243 (1981).
[29] M. P. Taylor, Liq. Cryst. **9**, 141 (1991).
[30] J. P. Straley, J. Chem. Phys. **57**, 3694 (1972); M. A. Cotter, Phys. Rev. A **10**, 625 (1974).

[31] In the case of perfect in-layer orientational order, it is also possible to construct a tilted smectic-C phase within this model. This is accomplished by rotating the spheroplatelets through a tilt angle θ about one of the two principle axes which are originally perpendicular to the smectic ordering axis (i.e., within the smectic layer the spheroplatelets remain parallel to each other and yet they are tilted with respect to the layer). However, it is found that such a tilted smectic phase of spheroplatelets is always unstable with respect to the untilted ($\theta=0$) version.

[32] R. Alben, J. Chem. Phys. **59**, 4299 (1973); Y. Rabin, W. E. McMullen, and W. M. Gelbart, Mol. Cryst. Liq. Cryst. **89**, 67 (1982); A. Stroobants and H. N. W. Lekkerkerker, J. Phys. Chem. **88**, 3669 (1984).